SAPIENZA
UNIVERSITÀ DI ROMA

Adaptive Deep Learning through Visual Domain Localization

Facoltà di Ingegneria Informatica
Corso di Laurea Magistrale in Artificial Intelligence and Robotics

Candidate
Gabriele Angeletti
ID number 1459796

Thesis Advisor:
Prof. Tatiana Tommasi
Co-Advisor:
Prof. Barbara Caputo

Academic Year 2016/2017

Abstract

The goal of Domain Adaptation is to minimize generalization error in those cases where the i.i.d. assumptions do not hold. In the context of computer vision, and image recognition in particular, there can be a variety of factors that influences the shift between training and test distributions: background, lighting conditions, resolution, translation, scale, etc. These factors can have a dramatic impact on test performance.

Although much more robust than previous learning technologies, deep learning still suffers from the domain shift problem. In this work we focus on cases where the domain shift has a spatial grounding and we extend standard Convolutional Neural Networks (CNN) with the aim of further minimizing their generalization error. Our method is particularly tailored for robotics applications where translation and scale variations are among the main causes of domain shift.

We show that our proposed technique outperforms previous state-of-the-art approaches across a number of benchmark datasets and baseline network architectures.

Contents

List of Tables

List of Figures

Table 1: Mathematical Notation

Symbol	Meaning
x	A scalar.
$\boldsymbol{x}$	A vector.
$\boldsymbol{X}$	A matrix.
X	A random variable.
$P(\cdot)$	A probability distribution.
net	The current state of a neural network.
$\hat{y}$	The output of a neural network.
θ	The set of parameters of a neural network.
$L(\cdot)$	A loss function.
$\Omega(\theta)$	A regularization function.
α	Learning rate parameter.
σ	An activation function.
$*$	The convolution operation.

Chapter 1

Introduction

After many decades of ups and downs, deep learning techniques recently produced unprecedented breakthroughs in complex areas like computer vision, speech recognition, and natual language processing.
Deep learning [19] is a subset of machine learning based on Artificial Neural Networks—statistical models loosely inspired by insights from neuroscience. Two were the main enablers for this revolution: the ever increasing availability of large labeled datasets and the terrific growth of computational power that took place in recent years. In particular, the advent of GPUs speeded-up by orders of magnitude the kind of computations needed by deep learning.

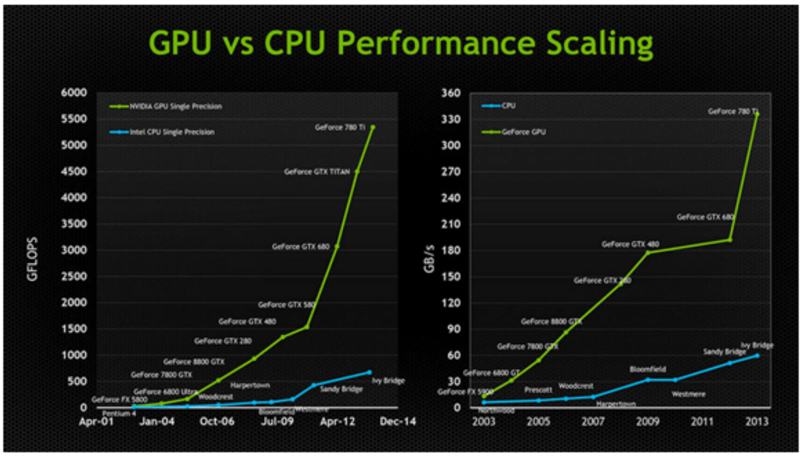

Figure 1.1: GPUs are optimized for parallel tasks, thus they are particularly suited to carry out computations like matrix multiplication, which is obiquitous in deep learning.

In computer vision in particular, state-of-the-art approaches for tasks such as image recognition, object detection and image segmentation all have

Convolutional Neural Networks (CNNs) [18] at their core: these are a specialization of the more general feedforward network architecture able to deal with data characterized by a grid-like topology.

Like the majority of machine learning technologies, also deep learning relies on the i.i.d. (independent and identically distributed) assumptions [35], according to which, the training and test samples are drawn from the same data generating process, i.e. by the same distribution.

The problem of dealing with settings in which the i.i.d. assumptions do not hold is known as Domain Adaptation [15], in which we seek to minimize generalization error in those situations in which there is a significant shift between the training distribution (also called *source domain* in the domain adaptation terminology) and the test distribution (called *target domain*).

Domain adaptation has important practical consequences, as solving this problem would imply being able to train offline models on huge dataset, and have them generalize well when deployed on the real-world. A typical scenario is that of a mobile app in which users take photos that are to be analyzed (e.g. classified, segmented, . . .) by an algorithm. These pictures are likely to come from a different distribution than that of ImageNet [33] for instance, and also are likely to be different between different users. The possibility of having a model (trained offline) capable of generalizing to these kinds of situations represents a practical, and useful, application of domain adaptation.

In the most recent computer vision literature there has been several attempts to combine deep learning and domain adaptation, however all the used experimental testbeds involve images with objects mainly appearing in the center and the learning procedure consider the images as a whole. In our work we want to deal with more realistic settings like that involved in robotics applications where pictures might be taken from very different angles and viewpoints and the domain shift is caused by significant variations in translation and scale. In these conditions, localizing the image parts more responsible for domain shift when applying the adaptation is highly beneficial. By following this intuition, in this work we propose a tailored adaptive deep learning architecture that outperforms existing baselines.

The rest of the thesis is organized as follows. Chapter 2 reviews basic concepts of machine learning and in particular summarizes the main elements of deep learning and convolutional neural networks. Chapter 3 focuses on domain adaptation presenting its main challenges as well as previous literature. In chapter 4 we describe our approach, the LoAd (Localized Adaptive) Network, describing the main components and the techniques it builds upon. In chapter 5 and chapter 6, experiments across a variety of robotics datasets and network architectures are reported. The thesis concludes with chapter 7 with a summary and a discussion on future research.

Chapter 2

Background

This chapter provides an overview of the problems addressed in this thesis work, as well as the main technologies upon which our approach is built. Section 2.1 is an introduction to the basics of deep learning, a branch of machine learning concerned with the study of Artificial Neural Networks (ANNs). This section draws heavily on [11].

2.1 Deep Learning

Introduction The hardware substrate of current digital information processors is very different from the biological substrate of the human brain. In fact, they are the opposite [2]. For this reason, many tasks that require effort and reasoning for a human to accomplish, such as chess, are pretty straightforward for machines, for those problems can be encoded into a set of formal rules which can then be solved algorithmically. Conversely, other kinds of tasks that humans do without even consciously reasoning about them are tremendously difficult for machines to accomplish. We find so easy to perform this kind of tasks that we don't even manage to explain how we do them. Encorporating the intuition and common sense that humans give for granted into machines is one of the holy grails of AI. In this context, one of the main innovations of deep learning, and of representation learning in general, in that of letting the machine learn by itself what the model of the world should be, instead of manually encoding knowledge into it. At the time of this writing, this is the most promising direction towards artificial intelligence.

History At first, it was believed that intelligent behavior could be achieved by hard-coding knowledge into the system by means of some formal language.

Reasoning would then be achieved through the use of inference rules, such as Modus Ponens. These were the so-called **Expert Systems** [14]. It was soon evident that the number of formal rules needed for intelligent behavior exceeds by several orders of magnitude the number of rules one could possibly write by hand.

This led to a major shift from deductive systems to inductive ones, where the machine itself *learns* to extract knowledge from data. By seeing a lot of input-output examples in the form $y = f(x)$ it would figure out the relationship f itself. This was the beginning of **Machine Learning** (ML). In ML, the algorithm does not see the raw data itself, but a higher level representation of it. Formally, a function $\phi(x)$ is provided which takes in input the raw data x and outputs a representation of x in the form of a numerical vector. This vector is then used to find the relationship between x and $y = f(\phi(x); \theta)$. In classical ML, the input representation is hand-crafted, that is the function $\phi(x)$ is manually designed by scientists and engineers often over the course of decades. This was a major drawback for many reasons:

- There is little transfer between different domains, such as vision and speech. That is, a function $\phi(x)$ that is found to work well on one specific domain, is not able to generalize to other ones as well.

- The majority of efforts and resources go into the feature engineering process itself. In most cases, it is more an art than a science.

- The goodness of the features entirely depends on human instinct. Many important features may simply be ignored or not discovered at all by scientist.

The natural evolution of this is to not only let the program learn the input-output relation $y = f(x)$, but also the input representation as well. That is, the algorithm learns both a suitable representation of the input $\phi(x)$, and then the relationship between this representation and the output $y = f(\phi(x))$. This research field is called **Representation Learning**.

Deep Learning is an extension of representation learning. The machine learns multiple levels of representations in a hierarchical fashion, where more complex concepts are built on top of simpler ones. Deep Learning is nowadays behind many state-of-the-art techniques in many research fields, like computer vision and speech recognition, and many believes it to be one of the most promising ways to reach human level artificial intelligence someday. In the following, we will provide a very concise introduction to the main concepts of deep learning. In particular, we will cover only a tiny subset of the whole field: *feed-forward (convolutional) neural networks* for *supervised* *learning* (classification). Thus, the setting is the typical one for classification problems: we have a *data set* of n samples, of which the i-th sample is $(X_i \in \mathbb{R}^K, Y_i \in \{1, 2, \ldots, C\})$, where X_i is a *tensor*, that is a multi-dimensional array, and Y_i is the class label for sample i. The task is to provide a model capable of predicting the correct class label $Y^{'}$ for a previously unseen instance $X^{'}$.

2.1.1 Feed-Forward Neural Networks

The feed-forward network can be thought of as a general framework in which different layers of processing units are stacked on top of each other. Each layer implements a function that takes in input the output of the previous layer.[1] A single layer can be viewed either as implementing a vector valued function or as a set of parallel processing units, each of which takes in input the outputs of the previous layer units, performs some sort of computation, and outputs a scalar value. The name neural networks stem from the fact that these models are loosely inspired by how the human brain works. In this regard, the parallel processing units in each layer perform a role analogous to that of neurons in the brain. However, the similarity between artificial and biological neural networks is very superficial, and NNs should not be seen as an attempt to perfectly mimic the human brain. The classical example of a feed-forward network architecture is the MultiLayer-Perceptron (MLP) [5], in which each layer implements an affine mapping of the input followed by an element-wise non-linear function:

$$h = \sigma(Wx + b) \tag{2.1}$$

Where $x \in \mathbb{R}^{m \times n}$ is the layer's input, $h \in \mathbb{R}^{m \times p}$ is the output, σ is the non-linearity (called the *activation function*) and $W \in \mathbb{R}^{n \times p}, b \in \mathbb{R}^p$ are the layer's parameters. The parameters W are called the *weights*; in MLPs there is a different weight for each pair of input-output units. The intercept of the affine mapping b is called the *bias*, because it represents the output of the layer when the input is zero. Regarding σ, there exists many non-linearities in the deep learning literature, some of the most popular are the *sigmoid or logistic* function, the *hyperbolic tangent (TanH)* and the *rectifier linear unit (ReLU)*:

$$Sigmoid(x) = \frac{1}{1 + e^{-x}}, TanH(x) = \frac{e^x - e^{-x}}{e^x + e^{-x}}, ReLU(x) = \max(0, x) \tag{2.2}$$

[1] Note that also the input and the output of the network are considered layers.

The layer $h = \sigma(Wx + b)$ described above can be thought of as a way of stretching and squashing space in order to project the input onto a new space in which it is linearly separable, that is, there exists a hyperplane separating the different classes. In the following depiction we can see such a layer in action:

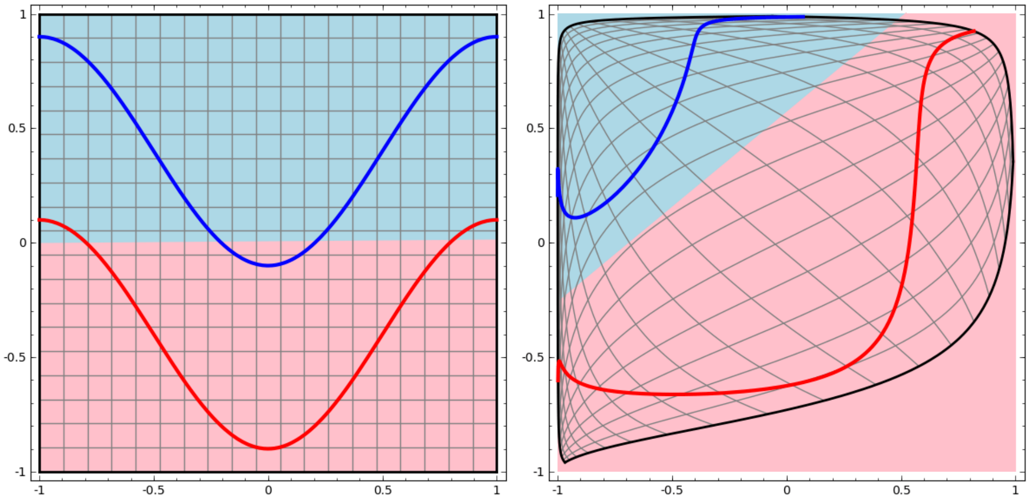

Figure 2.1: The original data (left) is not linearly separable, that is, there does not exists a hyperplane capable of separating the red curve from the blue curve. The transformation $h = \sigma(Wx+b)$ project the input x into a new space (right) where it's easy to find a separating hyperplane. Images taken from: http://colah.github.io/posts/2014-03-NN-Manifolds-Topology/

When we stack many such layers one on top of the other, we have a deep network. In particular, the input-output mapping defined by a MultiLayer-Perceptron with n layers is recursively defined as:

$$\hat{y} = W_n(\sigma(W_{n-1}(\sigma(W_{n-2}(\ldots\sigma(W_1x + b_1)\ldots)) + b_{n-2})) + b_{n-1}) + b_n \quad (2.3)$$

With W_1, b_1 denoting the parameters of the first layer and W_n, b_n the parameters of the last layer. The dimension of the first layers is constrained to be $(m, \cdot)$, with m number of inputs, while the dimension of the last layer is constrained to be $(\cdot, c)$, with c number of classes. The dimensions of all the other layers are hyper-parameters of the model that the designer of the architecture can arbitrarily chose. The number of layers n is also a hyper-parameter.

The output vector $\hat{y}$ has one entry for each class, and it can be thought of as the scores the network assigns to different classes. Since this vector can assume arbitrary values, it is typically followed by a function which converts the raw class scores into a probability distribution over classes, that is that normalizes the scores so that they sum to one. The most popular function used in the deep learning literature to do that is the **softmax** function:

$$softmax(z) = \left[\frac{e^{z_1}}{\sum_{i=1}^{c} e^{z_i}}, \ldots, \frac{e^{z_c}}{\sum_{i=1}^{c} e^{z_i}}\right], z = [z_1, \ldots, z_c] \tag{2.4}$$

Thus, the complete input-output mapping of the MLP is:

$$\hat{y} = softmax(W_n(\sigma(W_{n-1}(\ldots\sigma(W_1 x + b_1)\ldots)) + b_{n-1}) + b_n) \tag{2.5}$$

Now that we've defined our model, we need two more things: a definition of error and a procedure to learn from such errors.

The Loss Function The first thing to note is that the output of the model is a vector with c entries, one for each class. So we need to define the reference value y also as a vector with c entries. This is done by using the so-called *one-hot-encoding*, that is, class i is represented by a vector in which the i-th position is 1 and the other $c-1$ positions are 0. For instance, in a ten class classification problem, class 6 would be represented as $y_6 = [0, 0, 0, 0, 0, 1, 0, 0, 0, 0]$. Having both the model output $\hat{y}$ and the reference value y, we can define the loss function. The most popular choice for classification tasks in deep learning is the **cross-entropy** loss function, defined as:

$$L(y, \hat{y}; \theta) = -\sum_{i=1}^{c}[y_i \log(\hat{y_i}) + (1 - y_i)\log(1 - \hat{y_i})] \tag{2.6}$$

It is easy to see that for all the entries for which $y_i = 0$, only the second term contributes to the loss, and for the entry for which $y_i = 1$ (the true label), only the first term contributes to the loss. It can be shown that this expression is the result of applying the maximum likelihood principle to the point estimation in the space of functions that is performed by neural networks. That is, the cross-entropy loss function represents the log-probability of classes as given by the model. The previous equation is the cross-entropy loss for a single input sample. In deep learning (and more generally in machine learning), the loss is usually averaged over a number of samples, called a *mini-batch*. In this case, the loss becomes:

$$L(y, \hat{y}; \theta) = -\frac{1}{N} \sum_{i=1}^{N} \sum_{j=1}^{c} [y_{i,j} \log(\hat{y_{i,j}}) + (1 - y_{i,j}) \log(1 - \hat{y_{i,j}})] \tag{2.7}$$

Now we know how to compute the model's errors with respect to reference values. The last thing to cover is the design of a learning procedure, that is how to modify the model's parameters in order to reduce future errors.

The Learning Algorithm In deep learning, the most popular technique for minimizing the loss function is **gradient descent**. The basic idea is that the gradient of the loss function with respect to the model parameters gives us the direction of maximum increase of the loss. Hence, by updating the parameters in the opposite direction, we are effectively minimizing the error. Formally, the learning rule is the following:

$$\theta^{k+1} = \theta^{k} - \alpha \nabla L(y, \hat{y}; \theta) \tag{2.8}$$

Where α is a hyper-parameter of the algorithm that controls the step size in the direction of steepest descent. It is called the **learning rate** in the literature. This parameter is of fundamental importance in the optimization procedure, as its value often makes the difference between convergence and divergence of the minimization process. Equation (2.8) was the most basic version of gradient descent. Other techniques have been developed in recent years to overcome the major limitations of this scheme. The momentum [31] method provides a sort of short-term memory of recent updates to the optimizer and it helps smoothing the trajectory of minimization and improving speed of convergence. More recent methods like Adam [16] are more sophisticated, as they employs per-parameter adaptive learning rates.
Now we know how to modify the network's parameters in order to minimize the loss function, but how do we compute the gradients? It turns out there is a very computationally efficient algorithm which allows us to compute the partial derivatives of the loss with respect to the model's parameters. This algorithm is called **backpropagation**.

The BackPropagation Algorithm The BackPropagation algorithm [23] computes partial derivatives in a feed-forward neural network. Although this technique is mainly used in the context of neural networks optimization, the algorithm is general and can be used to differentiate arbitrary functions.
The reference value y is defined with respect to the output layer of the network, so it is easy to compute the gradient of this layer. Hidden layers instead

do not have target values, so their gradient cannot be computed directly. But we know that hidden layers influence the output of the last layer, because they provide the representation on top of which the output layer is built. BackPropagation uses this fact to recursively compute the gradients starting from the output layer and going backwards to the first hidden layer. Hence the name BackPropagation. In particular, BackPropagation cleverly uses the chain rule of calculus to compute the partial derivatives in previous layers. The chain rule of calculus basically states that if we have a nested function $z = f(y) = f(g(x))$, the derivative of z w.r.t. x is equal to:

$$\frac{dz}{dx} = \frac{dz}{dy}\frac{dy}{dx}$$

This is similar to the structure of equation (2.5). The full learning procedure of a MultiLayer-Perceptron is showed in Algorithm 1.

2.1.2 Convolutional Neural Networks

As we saw in the previous section, in the standard feed-forward net each layer is composed by an affine mapping followed by some non-linearity. But this is not the only way in which layers can be designed. There exists several kinds of feed-forward architectures, and in this section we will see what is arguably the most popular and successful example of specialization: the Convolutional Neural Network (abbreviated as CNN or Convnet).

CNNs are a specialization of the feed-forward network, particularly suited to work with data in which spatial information is important, like time series in one dimension and images in two dimensions. If we have to train a standard feed-forward net to classify images, the first thing we would do is to transform the 2D image into a 1D vector by concatenating together all the pixel values. By doing this we are clearly losing the spatial information relating the pixel to one another. Convnets instead are capable of fully exploit the spatial correlations between pixels.

More formally, a Convolutional Neural Network is a feed-forward network in which at least one layer uses the convolution operation.

The Convolution Operation

The convolution operation employed in deep learning (also called *cross correlation*) is a linear operation. In the case of two dimensional data, in particular images, the output at pixel (i, j) is a weighted linear combination of a neighborhood around (i, j). The set of weights is called the *kernel*. It is easy to understand this operation by looking at picture 2.2:

Algorithm 1 MultiLayer-Perceptron learning algorithm.
The **forward** function computes the output of the network given input x: $\hat{y} = f(x; \theta)$. The **backward** function computes the gradients of the loss function with respect to the model parameters. It starts with the gradient of the output layer, and then it propagates it backwards. The **update** function updates the parameters of the network according to the gradient descent update rule. The three functions must always be called in this exact order: forward → *backward* → *update*

```
Require: $net$, the network
Require: $(x, y)$, (input, target output)
function FORWARD($net, x, y$)
    $h[0] = x$                                  ▷ h is a tensor holding the outputs of all layers
    for $k = 1, \dots, d$ do                    ▷ d is the depth (number of layers)
        $a[k] = net.W[k]h[k-1] + net.b[k]$
        $h[k] = \sigma(a[k])$
        $net.a[k] = a[k]$
    end for
    $\hat{y} = h[l]$
    $J(\hat{y}, y; \theta) = L(\hat{y}, y; \theta) + \lambda\Omega(\theta)$      ▷ $\lambda\Omega(\theta)$ is the regularization term
    return $(\hat{y}, J(\hat{y}, y; \theta))$
end function
function BACKWARD($net, y$)
    $g = \nabla_{\hat{y}} J(\hat{y}, y; \theta)$                 ▷ gradient of the output layer
    for $k = l, \dots, 1$ do                    ▷ from output to input
        $g = \nabla_{a[k]} J = g \odot f'(net.a[k])$   ▷ gradient before the non-linearity
        $net.gradB[k] = \nabla_{net.b[k]} J = g + \lambda\nabla_{net.b[k]}\Omega(\theta)$
        $net.gradW[k] = \nabla_{net.W[k]} J = gh^{(k-1)T} + \lambda\nabla_{net.W[k]}\Omega(\theta)$
        $g = \nabla_{h^{(k-1)}} J = net.W[k]^T g$      ▷ propagate the gradients below
    end for
end function
function UPDATE(net)
    for $k = l, \dots, 1$ do
        $net.b[k] = net.b[k] - \alpha \cdot net.gradB[k]$
        $net.W[k] = net.W[k] - \alpha \cdot net.gradW[k]$
    end for
end function
```

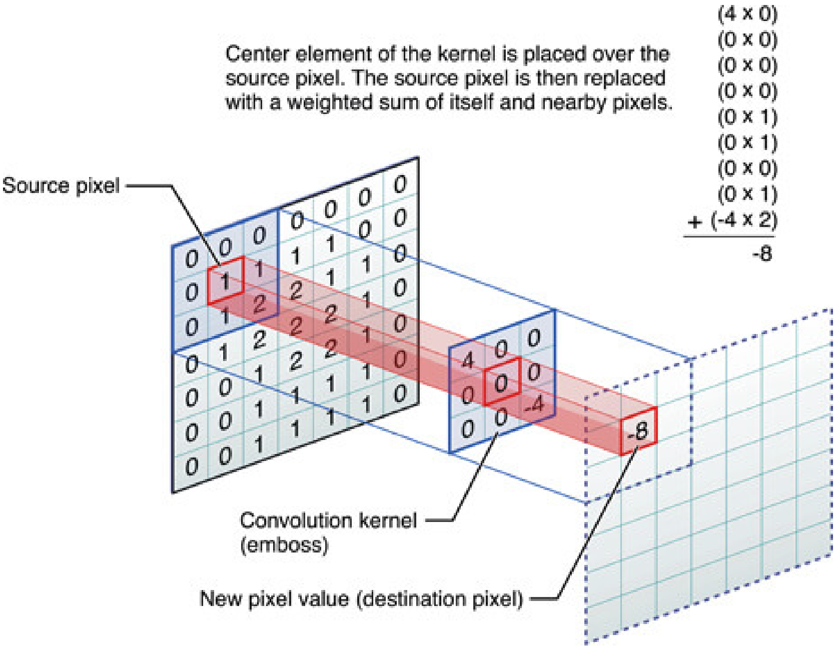
(4 x 0)
(0 x 0)
(0 x 0)
(0 x 0)
(0 x 1)
(0 x 1)
(0 x 0)
(0 x 1)
+ (-4 x 2)
-8
Center element of the kernel is placed over the source pixel. The source pixel is then replaced with a weighted sum of itself and nearby pixels.
Source pixel
Convolution kernel (emboss)
New pixel value (destination pixel)

Figure 2.2: The Convolution operation. Image taken from: https://developer.apple.com/library/content/documentation/Performance/Conceptual/vImage/ConvolutionOperations/ConvolutionOperations.html

More formally, the convolution operation for pixel (i, j) is defined by the following:

$$F(i,j) = (I * K)(i,j) = \sum_{w}\sum_{h} I(i+w, j+h)K(w,h) \tag{2.9}$$

Where I is the input image, K is the convolution kernel, and F is the output, also called *feature map*. The full feature map is defined by applying the previous operation for $i = \{1, \ldots, w\}$ and for $j = \{1, \ldots, h\}$, that is, the kernel is a window that slides over the entire image, computing the weighted combination at each pixel location. The kernel can be thought of as a specialized filter, which produces high responses to certain features of the input. For instance, a filter can produce a high response when it sees a vertical edge, or a blotch, and a low response in any other case.

Learning the kernels

The exists many techniques based on convolution and kernels to compute edges or other features in the input image, like the Sobel filter [10] for instance. The main difference with those approaches is that in Conv nets, the filters are not hand-crafted, but instead the network **learns** the values of the filters. In particular, in each convolutional layer, several kernels are computed in parallel, with each one specializing in the detection of a different feature. As a consequence of the hierarchical nature of deep learning, filters in low level layers specialize in the detection of low-level features such as edges and blobs, while high-level filters specialize in the detection of more high-level features, such as faces and animals.

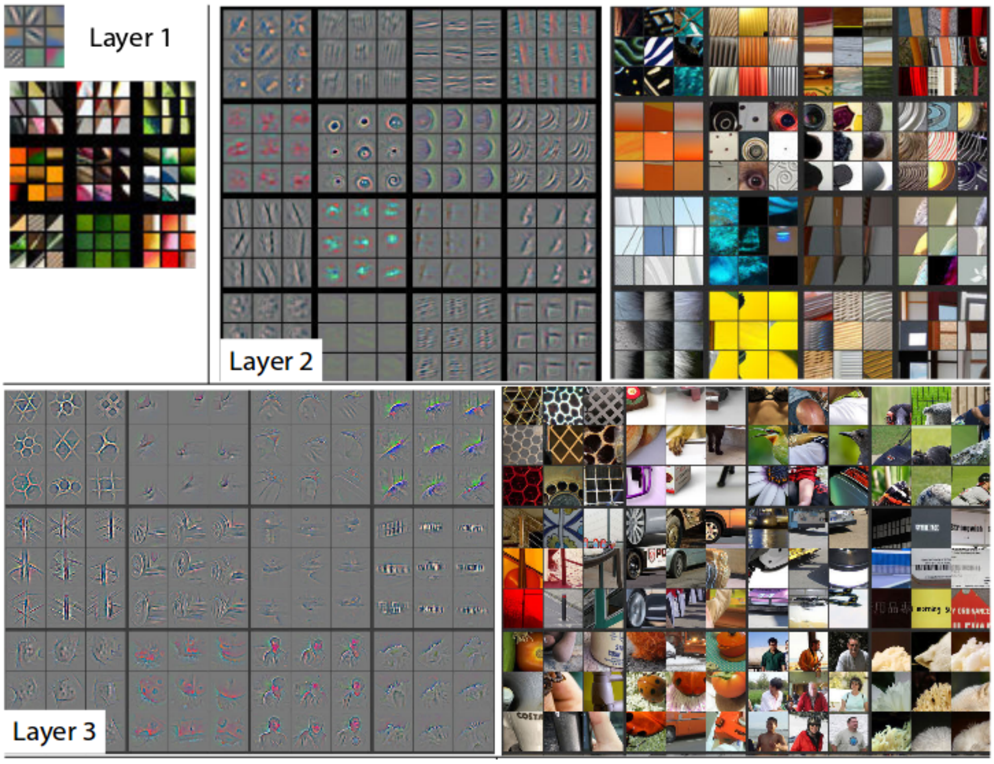

Figure 2.3: Visualizing Conv net filters, taken from [36]

In the next section we will see the other main building block of CNNs, namely the *pooling* operation.

Pooling in Convolutional Networks

In CNNs, a convolutional layer is usually followed by a pooling layer, that is a way of performing dimensionality reduction and improving the network overall robustness to input transformation. In particular, a pooling layer replaces the output of the network at pixel location (i, j) with a summary statistics of nearby pixels. Many statistics are usually employed in the deep learning literature [25]. The most popular is arguably max pooling [20], in which the summary statistic is simply the maximum value. Figure 2.4 shows how max pooling works.

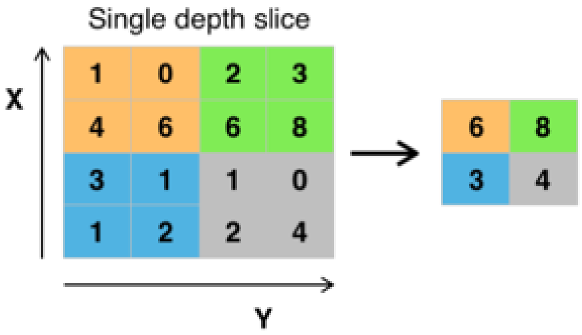

Figure 2.4: The max pooling operation.

It can be shown that the spatial pooling operation improves invariance to small translations in the input, i.e. if the input image is translated some pixels to the left or right, the output is still the same. This is a nice property to have when dealing with images, because we aren't usually interested in knowing precisely where a feature is located, but we are only concerned with whether the feature is actually present or not.

Advantages of Convolutional Networks

Convolutional Neural Networks have some unique features that make them particularly efficient, both from a computational viewpoint and from a computer vision perspective. The three main advantages of CNNs with respect to standard feed-forward networks are:

- **Sparse Interactions**: the feed-forward net is composed of affine layers $\sigma(Wx + b)$ where there is a different parameter for each pair of input-output units. Thus, each layer of the net has a number of parameters that is $O(m \times n)$, where m is the number of input units and n the number of output units. CNNs instead has a number of parameters that is $O(k \times w \times h)$, where k is the number of filters and w, h are respectively width and height of each filter. Since kernels are typically much smaller that the input, CNNs can have less parameters by orders of magnitude.

- **Parameter Sharing**: As we said in the previous point, feed-forward nets have a different parameter for each pair of input-output units. In

CNNs instead, each kernel is re-used over the entire input. This can be viewed as a parameter sharing technique, in which we have m kernels with the constraint that they have to share parameters. Of course, in practice, we have only one kernel that is used as a sliding window over the input, but thinking of it as a use of parameter sharing can give more insights into the effectiveness of CNNs.

- **Translation equivariance**: The convolution operation is naturally equivariant to translation, i.e. if the input is translated by a small amount of pixels to the left or right, the output is translated by the same amount. This is clearly a desirable property when dealing with images. This operation is not naturally invariant to other input transformations such as scaling and rotation, but CNNs as a whole can achieve such properties with appropriate mechanisms, albeit CNNs invariance is valid only for small transformations. In fact, making CNNs invariant to larger transformations is one of the main motivations behind this work.

Chapter 3

Related Work

In this chapter, we describe the domain adaptation problem in Section 3.1, highlighting the main challenges of the field. Then, in Section 3.2 we review previous literature and we describe the most recent state-of-the-art approaches.

3.1 Domain Adaptation

In the following, we will restrict our discussion of ML algorithms to the subset of supervised learning, represented by algorithms that learns a function $y = f(x;\theta)$ mapping an input vector x to an output vector y parameterized by θ.

Introduction Given a set of data x and their associated value y, supervised machine learning algorithms aim at modeling their functional relation $y = f(x)$ by minimizing the model's errors. The loss function $L(y, \hat{y}; \theta)$ evaluates the difference between the ground truth y and the predicted $\hat{y}$ on the basis of the model parameter θ. The main challenge in this task is the reduction of the generalization error: the optimized model should not only be able to describe the available training data but it should also make reliable predictions on new test data not available at training time.

The i.i.d. assumption A typical assumption done in machine learning settings is that the *training set* (X_{train}, Y_{train}) (the sample used to minimize L) and the *test set* (X_{test}, Y_{test}) (the sample used to evaluate generalization) are **i.i.d.**, namely independent and identically distributed. That is, each sample is independently drawn from the same underlying distribution $P(X, Y)$. The fact that samples are drawn independently is what allows us to write the loss function as a summation of a per-sample defined error function:

$$L_{sample}(y, \hat{y}; \theta) = \frac{1}{N} \sum_{i=1}^{N} L(y_i, \hat{y}_i; \theta)$$

The majority of learning algorithms operate under this assumption, which is usually a fairly good approximation. But there are cases in which this assumption does not hold, and this causes a significant drop between training and test performance.

Motivation Domain Adaptation [15] consists in the design of algorithms that work even when the i.i.d. assumption does not hold [1], i.e. when the distribution from which training samples are drawn is different from the one at test time. Domain adaptation has a slightly different terminology w.r.t. classical ML. In particular, the training distribution is called the *source domain* $D_S \sim P_s(X, Y)$, while the test distribution is called the *target domain* $D_T \sim P_t(X, Y)$. Typically, we assume that the source data is abundant and labeled, while the target data is either not or only partially labeled.
The setting with no annotations available for the target is known as unsupervised D.A. While if the target is partially labeled we are in the semi-supervised setting. This thesis work in particular focuses exclusively on the (harder) unsupervised setting.

Object Recognition In the context of object recognition, the domain shift can be very large and it can have a variety of different causes, which can also interact between each other in nonlinear ways. Factors such as background, lighting condition, resolution, translation, scale and rotation, all contribute to the shift in distribution between source and target. The goal of an object recognition system is twofold. Firstly, it is to find the factors that explain variation the data. Secondly, it is to disentangle the factors that are specific to one domain, e.g. the background, from the factors that are shared across domains, e.g. the objects themselves. A human is capable of performing this task accurately and reliably in a matter of milliseconds, but it has been beyond the reach of computer vision and machine learning algorithms for decades. We hope that the method presented in this thesis work provides a step in the right direction in order to improve object recognition systems and to provide promising directions of future research.

[1] Note that the assumption that samples are drawn independently is still valid.

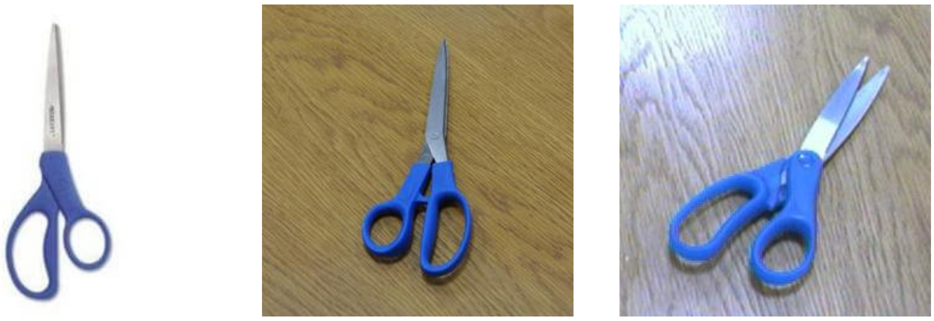

Figure 3.1: Examples of visual domain shift. The shift between the left and center images is clearly due to the background. The shift between the center and right images is due to resolution. In fact, the center image was taken with a high-resolution camera, while the right image was taken with a webcam.

Domain Adaptation In ML, the joint distribution between data and labels $P(X, Y)$ is unknown. In domain adaptation, we call the joint distribution of the source domain $P_s(X, Y)$, while $P_t(X, Y)$ is the joint distribution of the target domain. The i.i.d. assumption consists in a assuming that $P_s(X, Y) = P_t(X, Y) = P(X, Y)$. In Domain Adaptation instead, we have $P_s(X, Y) \neq P_t(X, Y)$. We can visualize what the implications of this fact are in figure 3.2.
The source data is drawn i.i.d. from the source distribution, while the target data is drawn i.i.d. from the target marginal distribution over X:

$$S = \{(x_i, y_i)\}_{i=1}^{N} \sim (D_S)^N$$
$$T = \{(x_i)\}_{i=1}^{M} \sim (D_T^X)^M$$

The goal is to build a classifier $f : X \to Y$ capable of making correct predictions about the target labels Y_t:

$$\theta^\star = \max_\theta P(Y_t = \hat{Y}_t | X_t; \theta)$$

Where $\hat{Y}_t = f(X_t)$ are the labels predicted by the classifier and Y_t are the true target labels, which we don't have access to.

3.2 Domain Adaptation approaches

Domain Adaptation is a fundamental problem in machine learning, and the need for techniques that works when $P_s(X, Y) \neq P_t(X, Y)$ is preminent in the

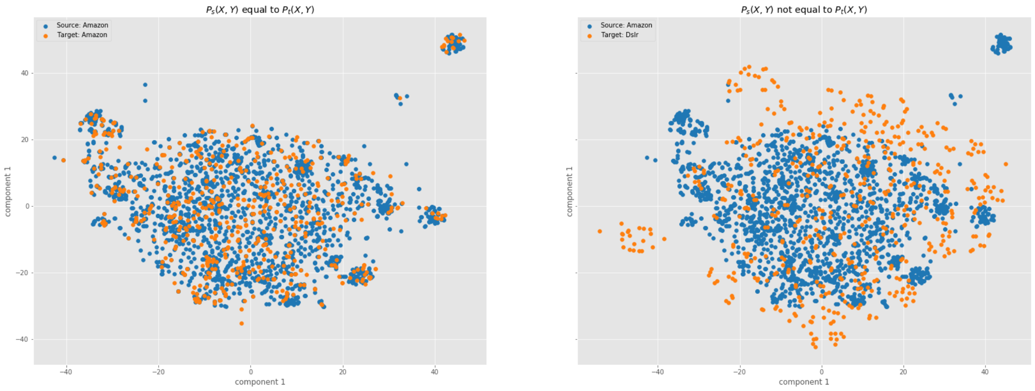

Figure 3.2: t-SNE [17] visualization of the features extracted from the Office dataset [24] using AlexNet [1]. When the source and the target distribution are the same (left), a classifier trained on the source data generalizes very well to the target data. When the i.i.d. assumption does not hold (right), the model will generalize poorly.

majority of practical applications. In computer vision in particular, there is a large number of factors which can cause the domain shift: background, lighting conditions, resolution and scale, position and orientation of the object of interest and so on. Various approaches to address the domain adaptation problem have been proposed in the literature. In the following overview of the domain adaptation literature, we will use the same distinction of [4] into shallow methods and the more recent deep methods, which employs deep learning models, in particular the deep convolutional networks described in Section 2.1.

3.2.1 Shallow Methods

In this context, shallow methods refers to those methods based on feature vector representations $\phi(X)$ extracted from the images with non-deep-learning methods.

Instance Weighting The earliest solutions to the domain adaptation problem go under the name of *Instance Weighting* approaches. The basic idea is that of assigning a different weight to each source sample in the computation of the loss. The definition of the weight varies based on the assumptions one makes about the source and target distributions. One possible approach is assuming that the conditional distributions of the labels given the same observation are the same, but clearly the marginal distributions of the observations are different. Formally:

$$P_s(Y|X = x) = P_t(Y|X = x) \text{ with } P_s(X) \neq P_t(X)$$

This assumption is called *covariate shift* and it is explored in depth in [28]. To solve the covariate shift problem, [28] weights each training instance with $\frac{P_t(X)}{P_s(X)}$, that is, the weight is the ratio between the likelihood of being a target and a source sample.

Feature Space Alignment Another class of techniques try to align source features with the target ones. A very simple method in this class is Subspace Alignment (SA) [7], where the alignment is made between the subspaces obtained by PCA reduction:

$$P_s = PCA(X_s, d) \qquad P_t = PCA(X_t, d)$$

$$X_s^{'} = X_s P_s P_s^T P_t \qquad X_t^{'} = X_t P_t$$

And then $X_s^{'}$ and $X_t^{'}$ are used in place of X_s and X_t.

Feature Transformation through metric learning Some domain adaptation approaches exploit metric learning solutions but in most of the cases they need labeled data both in the source and in the target domain. The only method that used this strategy in the unsupervised setting is DA-NBNN [34]. Its main idea was to iteratively replace the most ambiguous source example of each class by the target example for which the classifier (Naive Bayes Nearest Neighbor (NBNN)) is the most confident for the given class. It does this by iteratively learning a metric of the relatedness between the source and target domains.

3.2.2 Deep methods

The expression deep methods refers to all those approaches which are based either on fixed features extracted from a deep learning model or on the design of a novel deep network architecture which encorporates elements to solve the domain adaptation problem. One method worth mentioning in this respect is the Domain Adversarial Neural Networks (DANN) [9], which obtained state-of-the-art results on several benchmark datasets. It is called adversarial training because a part of the network is optimized in such a way to confuse another part of the network.

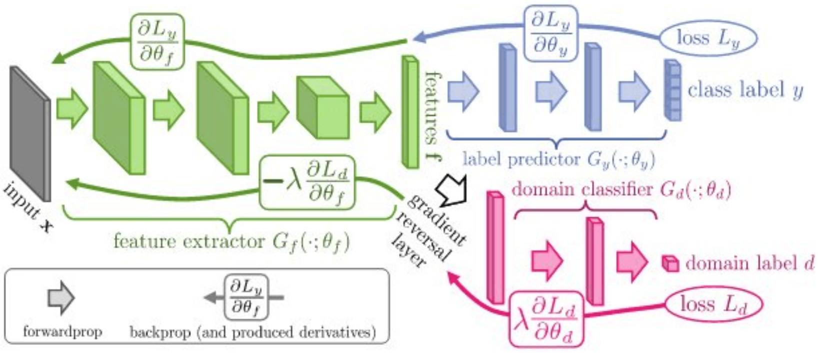

$\frac{\partial L_y}{\partial \theta_f}$
$\frac{\partial L_y}{\partial \theta_y}$
loss L_y
class label y
features f
label predictor $G_y(\cdot;\theta_y)$
$-\lambda\frac{\partial L_d}{\partial \theta_f}$
input x
domain classifier $G_d(\cdot;\theta_d)$
gradient reversal layer
feature extractor $G_f(\cdot;\theta_f)$
domain label d
$\lambda\frac{\partial L_d}{\partial \theta_d}$
loss L_d
forwardprop
$\frac{\partial L_y}{\partial \theta_f}$
backprop (and produced derivatives)

Figure 3.3: DANN Architecture. Image taken from [9].

DANN

The network is composed of three parts:

- **feature extractor**: this part of the network is trained to simultaneously optimize two objetives: learn features that are discriminant for the source classification task, and at the same time learn domain invariant features, that is, features that would increase the classification error of a binary domain classifier.

- **image classifier**: this is the classifier that carries on the main image classification task.

- **domain classifier**: this is the binary classifier that carries on the domain classification task between source and target. It is the adversary of the feature extractor.

DANN is not a novel architecture per se. Instead, it can be thought of as a method to extend existing networks to perform domain adaptation. One feature of DANN worth mentioning is that it is application-agnostic, namely it is general enough that it can be applied to different areas, such as computer vision, natural language processing and speech recognition. This is different with respect to our method, which is designed specifically for computer vision applications.

Chapter 4

The Local Adaptive Network

In this chapter we introduce our novel Local Adaptive Network that is able to discover the image parts more responsible of the domain shift and to perform a tailored adaptation across source and target samples.

This technique builds upon three methods:

1. We employ a modification of Grad-CAM [27] to generate what we call *domainness maps*, which tell us on a per-feature-map basis which regions in the image are discriminative between source and target domains.

2. Spatial Pyramid Pooling [13] is used to perform pooling at multiple levels in a parallel fashion. This can be useful when localization of the object in the image is an issue. It also generates fixed-length representations regardless of the input size.

3. Inspired by the Multiplicative Fusion approach presented in [22], we combine the information provided by the domainness maps with that coming from the feature maps. The maps inhibit domain-specific regions (regions that are discriminative for the two domains) and enhance domain-generic regions, thereby reducing the domain shift between source and target.

In the following, we review each of these components and we explain how they have been combined for our Local Adaptive Network.

4.1 Grad-CAM

Motivation Grad-CAM (Gradient-weighted Class Activation Mapping) [27] is a method for visualizing the spatial locations in an image that contributed

the most to the CNN's classification choice. The technique is applicable to a wide variety of tasks, ranging from image captioning to visual question answering to reinforcement learning, and also to a wide variety of CNN architectures.
Grad-CAM was designed as a visualization tool to better understand how CNNs reason and to improve their interpretability, which is a fundamental property to have for AI systems that wants to be deployed in the real world. In the context of this thesis work, we use this technique to visualize the spatial grounding of domain shift: looking for the regions more or less responsible for the difference across domains.

How it works Although visualizations can be extracted at any layer of the hierarchy, we opted for the last convolutional layer, because it is the best compromise between high-level semantics and spatial localization. The former is a general property of deep learning models: the further the layer from the input, the more high-level and meaningful the features extracted are. The latter is a property of convolutional feature maps, which are designed to retain as much spatial information as possible about the input. Fully-connected layers down the hierarchy do not have this property.
The high-level structure of the method can be seen in the following figure:

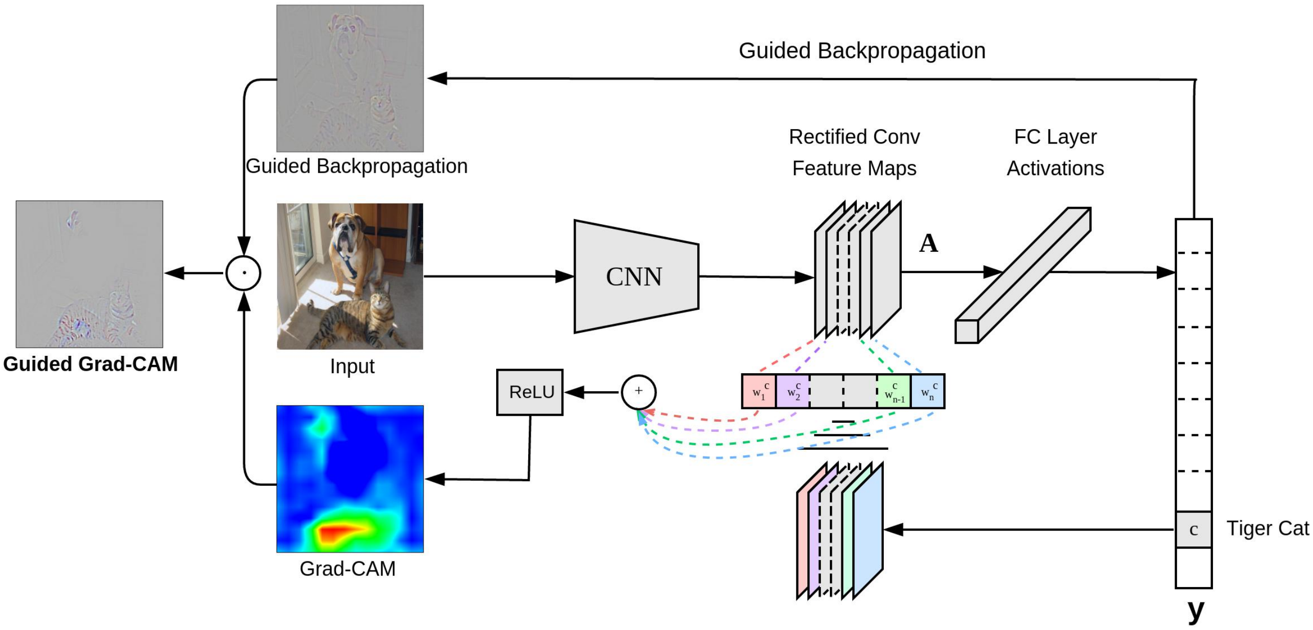

Figure 4.1: Grad-CAM Architecture, taken from [27]

Basically, the input image is forward propagated through the network in order to compute the softmax scores of the last layer, which we call $y^c = f(x)$, where $f()$ is the input-output network mapping. If we were training the network, at this point we would have computed the gradients of the last layer neurons with respect to some loss function, like cross-entropy. Instead, in Grad-CAM, we manually create these gradients. In particular, we set them to one for the neuron corresponding to the class of interest, while all the other neurons are set to zero.

$$\frac{\partial y^c}{\partial \theta_{output}} = [0, 0, \ldots, 1, 0, 0, \ldots]$$

Then, we backward propagate these gradients through the network until the last convolutional layer, where the Grad-CAM map is created. Assuming that the last convolutional layer feature maps are in $\mathbb{R}^{K \times H \times W}$, where H and W are respectively the height and the width of each feature map, and K is the number of feature maps (depth). The map that will be generated is thus in $\mathbb{R}^{H \times W}$. The generation procedure has multiple steps:

1. Compute the weight of each feature maps. We want a number measuring how much each filter contributed to the final score. It is therefore natural to compute this number as the derivative of the output gradients with respect to the weights of the filter. These derivatives are then global average pooled in order to get a single number:

   $$w_k^c = \frac{1}{Z} \sum_{i=1}^{h} \sum_{j=1}^{w} \frac{\partial y^c}{\partial F_{i,j}^k}, \tag{4.1}$$

   here w_k^c is the weight of feature map k with respect to target class c, while F is the feature map itself. We can see that the derivative is positive if an increase of the value of the pixel $F_{i,j}^k$ yields an increase of the value of y^c.

2. The Grad-CAM map is obtained by performing a rectified weighted linear combination of the forward feature maps:

   $$M^c = ReLU\left(\sum_{k=1}^{K} w_k^c F^k\right) \in \mathbb{R}^{H \times W} \tag{4.2}$$

The $ReLU()$ function simply set to zero all the negative values. The Grad-CAM technique uses this function to retain only the values that have a *positive* influence on the class decision. Once the Grad-CAM map is produced, it is then upsampled to the pixel space using bi-linear interpolation, then a heatmap is generated from the values and the heatmap is point-wise multiplied with the output of the Guided-BackPropagation procedure [30], to produce the final result called Guided-GradCAM.

4.1.1 Grad-CAM for domain localization

To perform domain localization with Grad-CAM, we replaced the 1000-units softmax of ImageNet CNNs with a single sigmoid unit, and we fine-tuned the network to perform a binary classification between source and target samples. Our rationale is that by applying Grad-CAM to this binary network we are able to determine which regions in the image are *domain-specific* (information contained only in one domain and not in the other) or *domain-generic* (information shared between domains). Having this clue on a *per-feature-map* basis, we are able to make source and target more similar at the representational level, by removing domain-specific locations and enhancing domain-generic ones. Figure 4.2 depicts two sample images along with their domain-specific and domain-generic heatmaps, obtained by summing the per-feature-map activations over depth.

Our domainness maps are actually generated using a subpart of the full Guided-GradCAM procedure. In particular, we used only Grad-CAM maps (without Guided-BackPropagation), and we retained the full *per feature-map activations*, instead of summing them across depth. Namely, in our method, equation 4.2 becomes:

$$M^c = ReLU\left(w_k^c F^k\right) \in \mathbb{R}^{K\times H\times W} \tag{4.3}$$

That is, instead of summarizing into a single map, we retain information about how each filter contributed to the decision of the class. This is crucial, as it enables us to enhance and inhibit filters with a greater precision.

4.2 Spatial Pyramid Pooling

Motivation As explained in Section 2.1.2, the max pooling operation is the most popular choice to perform dimensionality reduction in CNNs. Max pooling is a sliding window of a certain size in which for each window, the pixel with the maximum value is taken as output. Other summary statistics were employed in the literature, such as average pooling or sum pooling, but max pooling was found to work best in the context of object recognition [26]. After the last pooling layer, the resulting 3D tensor of dimension $C \times H \times W$

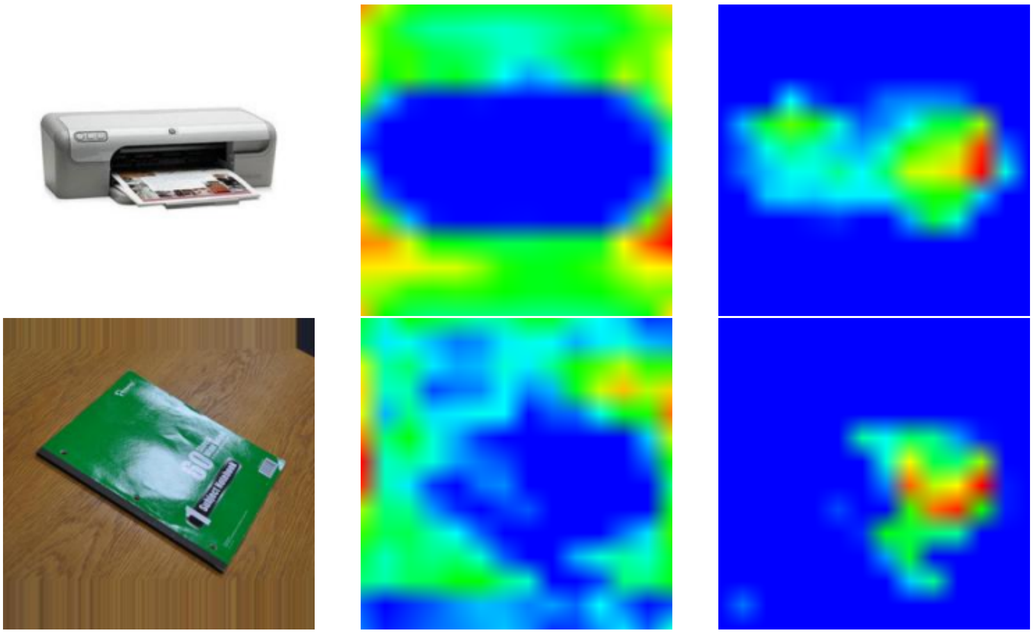

Figure 4.2: Examples of domainness maps. Both rows have: (left) original image, (center) domain-specific map, (right) domain-generic map. We can see that the domain-specific map captures information contained in one domain but not in the other, in this case the background. Domain-generic maps instead captures information shared between domains, in this case the objects themselves.

is flattened into a 1D tensor, and a series of fully-connected layers is placed on top of this layer. The are at least two problems with this architecture:

- Convolutional layers can deal with images of different sizes, but they will also produce outputs of different sizes. Fully-connected layers instead, only accept inputs of fixed size. Thus, the previous architecture cannot exploit this strength of convolutional layers.

- The designer should carefully choose the dimension of the pooling layers because, as we have seen in our experiments, this can have a major impact on the overall performance of the model. In particular we have seen that the last pooling operation is of particular importance when the object is translated or scaled by a large amount of pixels.

SPP-Net Spatial Pyramid Pooling (SPP) is a method that was used extensively by the computer vision community before the deep learning revolution. This paper [13] introduced the technique in the context of CNNs. Basically, a Spatial Pyramid Pooling operation is composed by multiple max pooling operations performed at different window sizes and then concatenated together in the depth dimension. This seemingly simple modification of the standard pooling layer has profound implications, such that:

- With a SPP layer as the last layer before the MLP, the network can take in input images of arbitrary sizes, scales and aspect ratios.
- The network is much more robust to translation and scaling of the input, because a pooling done at multiple levels is much able to capture such variations.
- The authors shown a small but consistent classification accuracy improvement over a large range of architectures and datasets.

Figure 4.3 is a depiction of how this layer works.

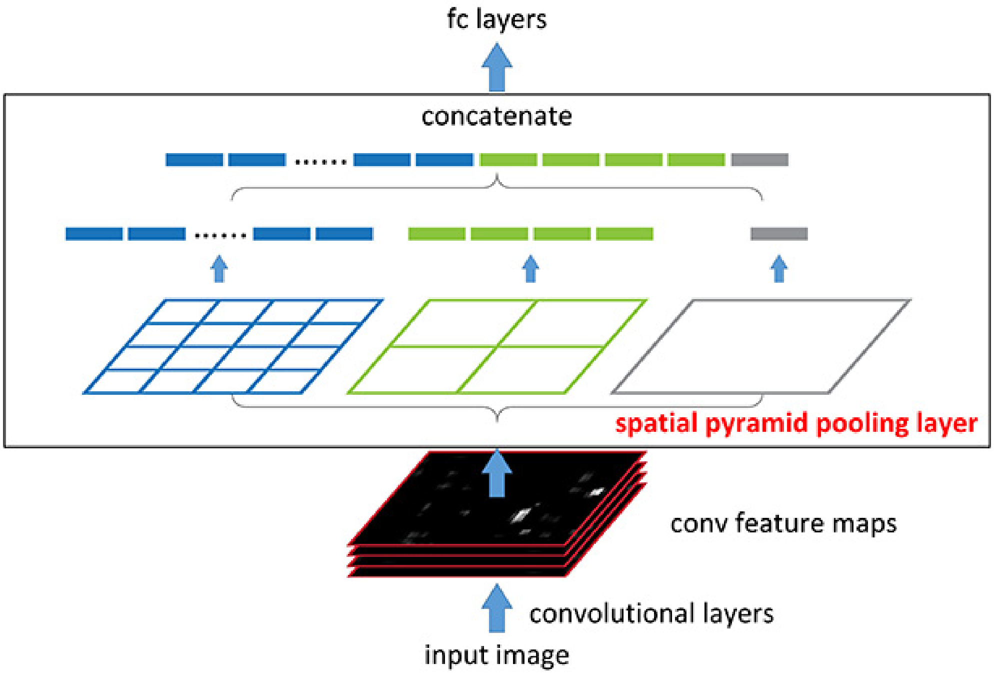

Figure 4.3: Spatial Pyramid Pooling layer. Image taken from: [13]

The pooling operation employed at each level is slightly different from the one we have described before. In particular, the one used here is called

Adaptive Pooling: instead of choosing the window size and the stride, we directly choose the output dimensions we want (say $n \times n$). From this, the window and the stride are automatically computed as $window = \lceil \frac{a}{n} \rceil$ and $stride = \lfloor \frac{a}{n} \rfloor$, where a is the dimension of the last conv layer feature maps. As a practical example, the VGG16 network [29] last conv layer feature maps have dimension $512 \times 14 \times 14$[1]. If we want an adaptive max pooling of dimension (4×4), the window and the stride are computed as $window = \lceil \frac{14}{4} \rceil = 4$ and $stride = \lfloor \frac{14}{4} \rfloor = 3$. Figure 4.3 has a SPP layer with three levels: $(4 \times 4)(2 \times 2)(1 \times 1)$. We can easily compute the (fixed) output dimension of this layer. For instance, with the VGG16 network, the output size is: $(512 * 4 * 4) + (512 * 2 * 2) + (512 * 1 * 1) = 10752$, so we can place a fully-connected layer on top of this SPP and we can be sure that the dimension will be the same regardless of the input size.

During our experiments we observed that the size of the window in the pooling operation is an important factor to take care of when dealing with a domain shift problem. Usually, one takes whatever dimension was chosen for the baseline network (AlexNet or VGG) and keeps it fixed. However, we adopted the original SPP strategy with the aim of testing different window sizes and we effectively verified that results can vary significantly based on this parameter. As a consequence, we believe that this is an important factor when dealing with learning across domains, and it cannot be considered simply fixed. The experiments empirically proved this intuition showing that this is a parameter that has to be carefully optimized.

4.3 Multi-cue Multiplicative-Fusion

Motivation Learning by combining multiple information is one of the hallmarks of human intelligence and it is an important ability for any artificial agent. Many works has been dedicated to techniques for the integration of multiple cues. In particular, two approaches has been proposed in [22], starting from CNN architectures in the context of action recognition. The first technique, which they called *Feature Amplification*, consists in an element-wise (hadamard) product between two sources of information: the first was the CNN feature maps and the second was the optical flow [8] information. The rationale was that through the multiplication, CNN feature maps information would detect important features for the action recognition task,

[1] these are the output dimensions when the input image is 224×224. For bigger (smaller) images, a would be greater (less) than 14. However, using adaptive pooling, the output dimension will be $512 \times 4 \times 4$ regardless of the input size.

and optical flow information would amplify (cancel out) important regions in the feature maps with respect to the task of detecting motion. The second method, named *Multiplicative Fusion*, combines the feature maps coming from two different CNNs into a merged representation which is then propagated through the fully-connected layers. In particular, a new layer linearly combines the feature maps and the coefficients of the combination are considered as learnable parameters. Figure 4.4 shows the multiplicative fusion architecture.

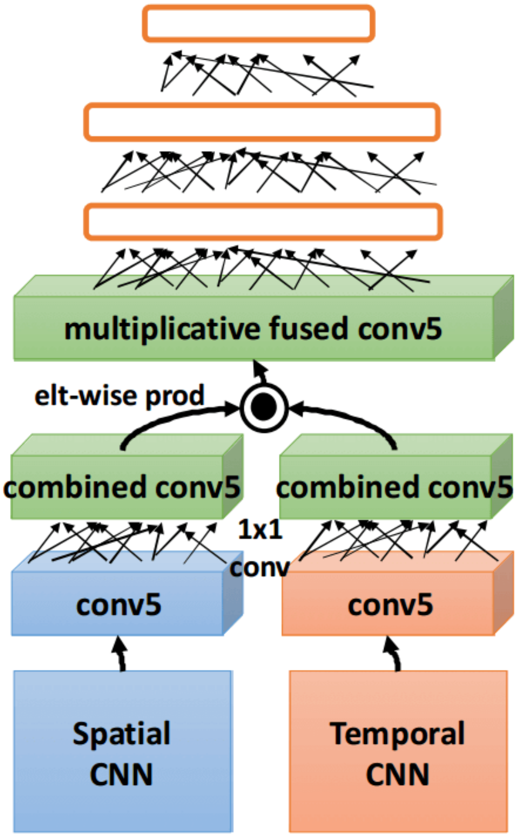

Figure 4.4: Multiplicative-Fusion architecture. Image taken from [22]

4.3.1 Local Adaptive Convolutional Neural Network

Before introducing the details of our Local Adaptive Network (LoAd CNN) let's briefly recap our domain adaptation task and setting. We have two datasets which were drawn from two different distributions: the *source* dataset (X_s, Y_s) was drawn from $P_s(X, Y)$, and the *target* dataset (X_t) was drawn

from $P_t(X)$, with $P_s \neq P_t$. Our learning task is to design a model that learns how to infer Y_t given (X_s, X_t, Y_s).
Our method can be summarized in the following way:

1. We train a CNN with a binary classifier on top of it to discriminate between source and target samples. The source samples are assigned a label of 0, and the target samples a label of 1. The CNN ends with a single sigmoid unit, which outputs the probability of the sample being a target sample:
$$P(Y = 1|X) = \hat{y}$$
This model is trained using the binary-cross-entropy loss function and stochastic gradient descent. Note that we are in the unsupervised domain adaptation setting and the procedure is completely agnostic of the target object labels.

2. We use the Grad-CAM technique on the binary domain classification network to generate activation maps. In particular, for each image, we generate a domainness map of the regions that would make the classifier change its decision, from source to target or vice-versa. The activations are of the last convolutional layer, which has a more compact and meaningful representation, as the author of Grad-CAM also pointed out.

3. The domainness maps are integrated into a final CNN that performs object classification on the source data. The final architecture can be seen in figure 4.5. From the input layer to the last convolutional layer, the architecture is the same as a standard CNN. Then, the output feature maps are duplicated: one copy is kept as in its original form, the other is multiplicatively fused with the domainness map. We use Spatial Pyramid Pooling for each of the two branches, motivated by our discussion in Section 4.2. The two branches are then recombined by concatenation producing an enriched feature with an highlight on the domain generic parts of the images.

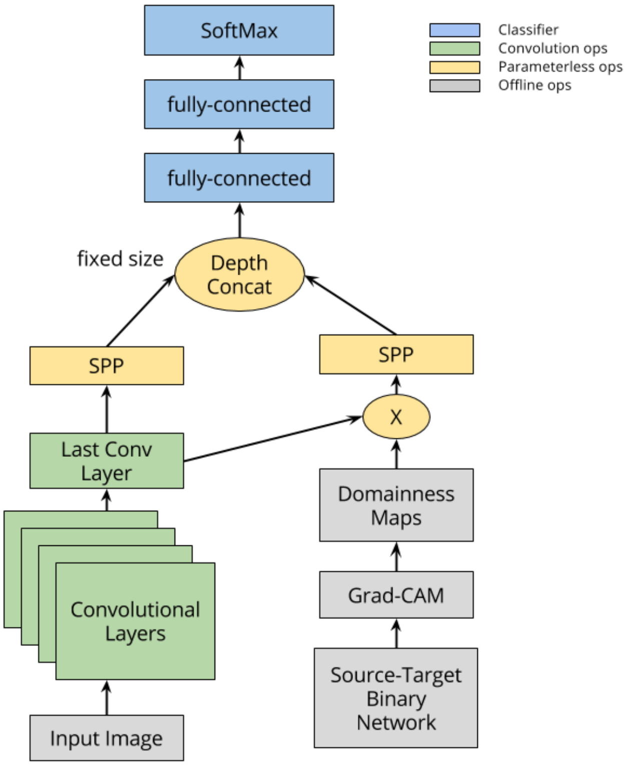

Figure 4.5: Local Adaptive CNN.

Chapter 5

Experiments

5.1 Implementation

We use Torch7 library [3] for implementation. The LoAd building blocks, besides the standard layers, are the element-wise multiplication and the depth contact operation, which are already available in Torch7. Regarding Grad-CAM, we start from the code provided by the authors [12] and we modify it as discussed in Section 4.1.1. We implement the Spatial Pyramid Pooling layer as an extension of Torch7, and we build the computational graph to compose the building blocks into the overall end-to-end architecture.

For each experiment setup, we train and test three different network configurations. All three variants starts from a baseline network pretrained on the *ImageNet* dataset [33]. In the first configuration (which we call Softmax), we replace only the last layer of the network with a new layer with dimension equal to the number of classes in the dataset. We train only this last layer, keeping all the other parameters frozen during training. In the second network (Spp), we remove all the fully-connected layers, as well as the last Max Pooling layer. We replace the latter with a Spatial Pyramid Pooling layer, and we add new fully-connected layers on top of it. The third network is LoAd, whom architecture is discussed in Section 4.3. Note that in Spp and LoAd the substitution of the fully-connected layers is necessary, as in a feed-forward network the removal of layer i constrains us to remove also layers $i + 1$ to n.
With this configuration of networks, we are able to verify the effectiveness of each component of the LoAd Network. In one experiment setting, we also compare our technique against state-of-the-art approaches.

5.2 Experiment settings

5.2.1 Baseline Networks

In our experiments we use two baseline networks. The first is *Alexnet* [1], winner of the ILSVRC 2012 competition and the responsible for the recent deep learning revolution in computer vision. The paper introduced many interesting innovations, most notably the use of Graphics Processing Units (GPUs) to train neural networks with millions of parameters at large scale, a method to reduce overfitting known as Dropout, and the use of the Rectified Linear Unit (ReLU) activation function. The second network is VGG16 [29], winner of the ILSVRC 2014 competition. VGG16 is much deeper than Alexnet, in fact Alexnet has 5 convolutional layers and 3 fully-connected layers, while VGG16 has 13 convolutional layers and 3 fully-connected layers. The use of two baseline networks improves the reliability of our findings.

5.2.2 Training procedure

Each network is trained using the same set of hyperparameters, established by using a validation set to search over a grid of possible values. The parameters of the first f layers are frozen, where $f = 22$ for AlexNet (Softmax), $f = 38$ for VGG16 (Softmax), $f = 5$ for AlexNet (Spp and LoAd), $f = 12$ for VGG16 (Spp and LoAd). The parameters of layers $f+1$ to g are not frozen, but they are set with a small learning rate $\alpha_{f+1,g} = 10^{-5}$ (Spp and LoAd) and $\alpha_{f+1,g} = 0$ (Softmax). g is the number of layers that are retained from the ImageNet baseline. The parameters of layers $g+1$ to n have a higher learning rate $\alpha_{g+1,n} = 10^{-3}$ (Softmax) and $\alpha_{g+1,n} = 5 \times 10^{-4}$ (Spp and LoAd). Also, for all the layers that are trained from random initialization, a weight decay of $w = 5 \times 10^{-4}$ is used as a regularizer. In Spp and LoAd, fully-connected layers have dimension $2048 \rightarrow 2048 \rightarrow 15$ for AlexNet and $4096 \rightarrow 2048 \rightarrow 15$ for VGG16, and they uses dropout with $p = 0.6$.

The optimizer used in the training procedure is Stochastic Gradient Descent with Momentum [31]. The momentum parameter is set to 0.9, with nesterov momentum [21] enabled. We use a batch size of 256 for AlexNet and 16 for VGG16 (due to the high memory footprint of this network). Training was performed in parallel on multiple NVIDIA Titan X GPUs.

5.2.3 Datasets and Metrics

We evaluate our LoAd on two variants of the iCub World dataset [32], which we call respectively iCW-translation and iCW-scale. Both datasets have two domains. As the names suggest, in the former case the shift between the two domains is caused by large object translations, while in the latter it is caused by scale variations. It is worth noting that, as discussed in Section 2.1.2, CNNs are known to handle some degree of scale and translation invariances. However, using a network structure specifically designed to handle such invariances have been shown to be more successful in many tasks [13]. In both datasets, one domain is composed by 4500 images and the other one by 3000 images. These are rather small datasets for data-hungry deep learning models, hence the choice of starting from ImageNet baselines. For iCW-translation, we also compare against prior state-of-the-art approaches.

To measure performance, we train each network over one domain and use the other domain as the test set, measuring classification accuracy. In order to improve statistical robustness, we run all the experiments 5 times, and we report mean and standard deviation of the results.

5.2.4 The iCub World dataset

The iCW Transformations dataset [32] contains images with objects from 15 categories, acquired through a robot camera. Each object is acquired while undergoing isolated visual transformations, in order to study invariance to real-world nuisances. A human operator moves the object holding it in the hand and the robot tracks it by exploiting either motion cues or depth cues. Different datasets are available depending on the object transformation carried out by the human. We will use two different variants of the iCW Transformations dataset:

- **Translation**: The human moves in a semi-circle around the iCub robot, keeping approximately the same distance and pose of the object in the hand with respect to the cameras. We use only images taken at the extreme of the semi-circle, thus the object appears either at the left of the image or at the right. Another cause of domain shift is that the background changes dramatically, while the object appearance remains the same.
- **Scaling**: The human moves the hand holding the object back and forth, thus changing the object's scale with respect to the cameras. In this case the two domains are again defined by keeping the images at the extreme of the object movement: far or close to the camera.

For each of the two variations the classes are perfectly balanced, namely each one has the same number of samples. Each dataset has two domains, which are both in turn considered as source and target. In figure 5.1, we can see a random sample of images from the dataset.

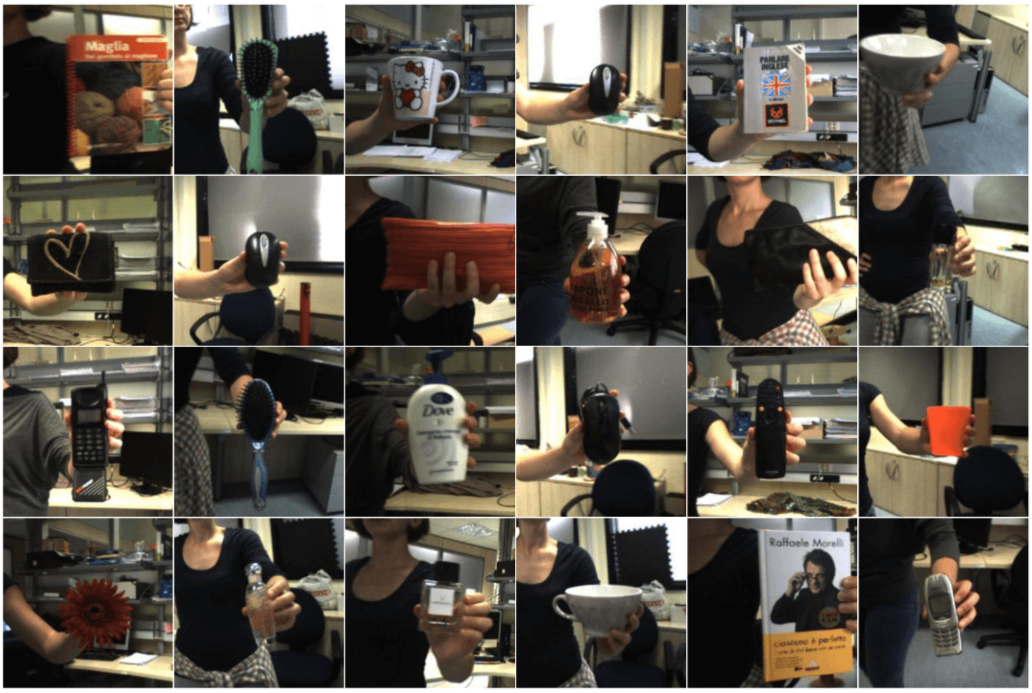

Figure 5.1: Random sample from the iCubWorld dataset.

Domain Shift The first thing to do is to verify if the iCW dataset actually represents a domain adaptation task. That is, we should measure the domain shift in the dataset. In the domain adaptation literature, this is usually done in the following way: we train a classifier on 80% of the source domain, and we test it both on the remaining 20% and on the target domain. The absolute difference of performance gives a rough quantitative measure of the domain shift. Intuitively, the more the performance difference, the more the two datasets were generated from different distributions. The following process is employed to measure this domain shift. First, image features are extracted at the second fully-connected layer of the VGG16. This gives a feature vector of 4096 entries for each image. We then run a Linear Support Vector Machine classifier [6] on top of these features. Results for both iCW translation and iCW scale are shown in Table 5.1.

In both datasets, there is a clear domain shift between the two domains. Also, by looking at Table 5.1, we can also see for instance that the task Scale 1 → Scale 2 is much more difficult than the opposite one. This might be

	S (80%) → S (20%)	S (80%) → T	Difference
Left 1 → Left 2	99.67	59.23	40.44
Left 2 → Left 1	99.83	62.47	37.36
Scale 1 → Scale 2	100.00	26.54	73.46
Scale 2 → Scale 1	99.67	40.98	58.69

Table 5.1: iCW domain shift measure. *S* stands for Source. *T* stands for Target. $X \to Y$ means that the SVM is trained on X and tested on Y.

because Scale 2 images contains information that helps the classifier also on Scale 1, but the opposite is not true.

Having seen that there is indeed a domain shift between the domains, in the next paragraph we compare our method both with standard transfer learning techniques and with the state-of-the-art Domain-Adversarial Networks [9].

Results

In the following tables we report the results of our experiments. In particular, we report the percentage of classification accuracy: the fraction of correctly annotated samples over the total cardinality of the target set. We can see that our method LoAd outperforms all the other techniques by a significant margin.

	Left 1 → Left 2	Left 2 → Left 1	Average
Softmax	50.41 ± 0.98	54.01 ± 0.59	52.21
Spp	63.55 ± 1.49	61.15 ± 0.69	62.35
DANN	63.20	42.93	53.07
LoAd	$\mathbf{67.35 \pm 0.97}$	$\mathbf{61.75 \pm 0.54}$	**64.55**

Table 5.2: iCW Translation Alexnet Results.

Besides observing the final classification accuracy of our LoAd network, we also verified that the features learned with our architecture are more robust to domain shift than that obtained through standard CNN without adaptation. Namely, we train a binary classifier to tell which distribution (source or target) samples were drawn from. Intuitively, if the distributions are the same, we should expect a classification accuracy of $\sim 50\%$, whether if the distributios are different, we should expect an accuracy of $\sim 100\%$. This

	Left 1 → Left2	Left 2 → Left 1	Average
Softmax	62.15 ± 0.94	64.74 ± 0.92	63.44
Spp	75.14 ± 1.09	75.91 ± 1.26	75.53
DANN	76.43	54.60	65.52
LoAd	$\mathbf{78.17 \pm 0.66}$	$\mathbf{77.30 \pm 0.80}$	**77.73**

Table 5.3: iCW Translation VGG16 Results.

	Left 1 → Left2	Left 2 → Left 1	Average
Softmax	18.20 ± 0.71	27.45 ± 1.23	22.83
Spp	25.77 ± 0.88	30.52 ± 0.60	28.15
LoAd	$\mathbf{29.68 \pm 1.52}$	$\mathbf{31.43 \pm 0.49}$	**30.56**

Table 5.4: iCW Scale Alexnet Results.

	Left 1 → Left 2	Left 2 → Left 1	Average
Softmax	30.85 ± 0.67	49.88 ± 0.73	40.36
Spp	35.69 ± 1.08	49.85 ± 1.38	42.77
LoAd	$\mathbf{42.16 \pm 1.09}$	$\mathbf{50.69 \pm 0.96}$	**46.42**

Table 5.5: iCW Scale VGG16 Results.

is indeed the case, as we've verified experimentally. What we would like to verify however, is if LoAd actually reduces the performance of such a binary classifier.

	iCW Translation	iCW Scale
ImageNet	96.67	97.87
Softmax	98.87	99.20
LoAd	**93.03**	**95.28**

Table 5.6: Domain shift reduction caused by LoAd. The binary classifier is a Linear SVM trained on top of features extracted from VGG16. Lower is better.

As the results in Table 5.6 shows, LoAd actually reduces the performance of the classifier (albeit by a little amount), hence making the two distributions more similar.

Chapter 6

Comparison

6.1 Comments on LoAd

The results of our experiments on the iCW dataset show that our method improves the object localization invariance of CNNs, thereby improving the performance of object recognition systems. The method can be used as an extension of any CNN, with no requirements on the baseline architecture. LoAd can be seen as an attention mechanism that allows the network to focus mostly on the regions of an image that are shared across domains, thus providing higher layers with a representation in which two domains are more similar.

We also argue that tuning the dimension of pooling layers can be an effective way of including *prior knowledge* about the localization of a dataset. If objects are centered and cover the majority of the image, there won't be much noise, and a smaller window size will retain more useful information. Conversely, if the object covers a small region of the image, there will be much noise. In those cases, a bigger window size might be appropriate, in order to drop useless information. We run experiments with the Spp configuration as described in 5.2.1, changing the dimension of the Spatial Pyramid Pooling layer. We see that in those cases where there are large object transformations, in particular translation and scale, a different dimension of the last pooling layer can make a difference in classification accuracy by as much as $\sim 10\%$. The pooling operation throws away a lot of information about the location in which a feature occurs. Therefore we speculate that carefully tuning the dimension of pooling layers, as demonstrated by our experiments, has the potential to bring many improvements in object recognition and detection systems based on CNNs.

6.2 State-of-the-art comparison

6.2.1 Accuracy

In Section 5.2.4 we compare our LoAd method against the state-of-the-art approach of Domain-Adversarial Neural Networks (DANN) [9]. LoAd outperforms DANN on all the variants of the iCW dataset by a significant margin. This is due in part to our discussion in Section 6.1 about tuning the dimension of the last max pooling layer, and in part to the fact that LoAd improves object localization in the presence of large object transformation, through the introduction of what can be thought of as an attention mechanism. However, we are not saying that LoAd is a better method than DANN, but only that it works better in those cases when object localization is an issue. In fact, we test both LoAd and DANN on a popular benchmark dataset in the domain adaptation literature, the Office 31 dataset [24]. This dataset contains objects from 31 categories belonging to three different domains: (1) Images taken from amazon.com, (2) Images taken with a high-resolution camera, (3) Images taken with a low-resolution webcam. In this setting, the domain shift is mainly caused by changes in background and resolution, while there are no changes in object localization, the object being almost always at the center of the image. In this adaptation task, LoAd was not able to outperform DANN on average, albeit it provides better performance on four out of the six adaptation tasks. This proves that LoAd, while performing best in the presence of a strong object localization, is also capable of providing almost state-of-the-art performance when this is not the case. As a last note, we find that LoAd works only in those cases where source and target domains are *different but related*. In fact, we test LoAd on datasets with a huge domain shift, and we find that our method performs poorly. However, this is also true for the other approaches. This shows that adaptation between completely different domains is still out of reach for current CNNs.

6.2.2 Size

Another point of comparison between LoAd and DANN regards the size of the model, i.e. the number of parameters. Both methods are extensions of baseline networks, but since LoAd does not reuse the entire architecture, it has a much lower number of parameters. The size (in number of parameters) of the two baseline networks used in this thesis work is 60×10^6 for Alexnet and 138×10^6 for VGG16. DANN replaces the last layer of the baseline network and it also adds two fully-connected layers for the domain regressor component. This leads to a size almost equal to that of the original model,

61×10^6 for Alexnet and 139×10^6 for VGG16. LoAd instead, replaces all the fully-connected layers in the baseline network with layers of lower dimension, thereby reducing the size of the model by a lot. In fact, LoAd size is 24.5×10^6 for Alexnet and 125.5×10^6 for VGG16. For Alexnet in particular, LoAd size is almost one third the size of the original model and that of DANN. This leads to a much better memory footprint and greater efficiency from a computational view-point.

Chapter 7

Conclusions

We design a method to tackle the increasingly important problem of domain adaptation, that is the problem of taking a machine learning classifier trained on a dataset and making it work on a different-but-related dataset, for which no labels are available. We describe the foundations upon which our method builds, and state-of-the-art approaches present in the literature. We provide experimental evidence across a range of datasets and network architectures that our method is an improvement over standard architectures, and it is also able to achieve state-of-the-art performance, while using very few parameters with respect to other methods. We argue that our work points out the importance of localizing *domain-generic* and *domain-specific* regions at a representational level, and that the use of this information can make the source representation more similar to the target representation.

7.1 Take home messages

We performed many experiments, and tried lots of approaches, and we learned many things along the way. One thing is that if we carefully tune the dimension of the latest pooling layer, we can achieve much greater performance (in fact, in some settings, we achieve a 10% improvement in test accuracy). Another thing is that with deep learning model the size of the dataset is really a fundamental issue: methods that work well when the dataset is big enough often do not work at all when the dataset is small. One should carefully tune the model capacity with respect to the dataset at hand, because with deep networks, overfitting is often around the corner. We also learned that domain adaptation is a hard problem that is yet to be solved: despite the huge successes that deep learning methods have achieved in computer vision over the last few years, a model trained on one dataset and tested on a different one continues to yield very low performance. Some also argue [37] that deep networks do not in fact learn semantically meaningful features, but instead they simply memorize entire datasets. With the advent of deep learning, we traded interpretability for performance, and we still know very little about how these models really work. Much more work needs to be done in deepen our understanding of deep neural networks.

7.2 Future work

We think that a promising future direction of this work would be to make the *domainness maps* created by a generative model: that is, by replacing the use of the Grad-CAM procedure with a generative network that is embedded in the network. In this way, instead of having two learning processes that are carried out in a sequential manner, one would have a single end-to-end architecture jointly trained in one step. Besides reducing the computational burden of our method, we also argue that this would increase the quality of the produced maps.

Currently, we are only relying on the domain localization to reduce the domain shift. This means that our approach can be easily integrated with other existing DA solutions. In this way, we would not only create a procedure that only attend domain generic areas but it is also able to reduce possible domain gaps still present in those areas.

Bibliography

[1] Geoffrey E. Hinton Alex Krizhevsky Ilya Sutskever. "ImageNet Classification with Deep Convolutional Neural Networks". In: (2012).

[2] MA Anusuya and SK Katti. "Superficial Analogies and Differences between the Human Brain and the Computer". In: *IJCSNS* 10.7 (2010), p. 196.

[3] Ronan Collobert, Koray Kavukcuoglu, and Clement Farabet. "Torch7: A Matlab-like Environment for Machine Learning". In: *NIPS* (2011).

[4] Gabriela Csurka. "Domain Adaptation for Visual Applications: A Comprehensive Survey". In: *CoRR* abs/1702.05374 (2017). URL: http://arxiv.org/abs/1702.05374.

[5] George Cybenko. "Approximation by superpositions of a sigmoidal function". In: *Mathematics of Control, Signals, and Systems* 2 (1989).

[6] Rong-En Fan et al. "LIBLINEAR: A library for large linear classification". In: *Journal of machine learning research* 9.Aug (2008), pp. 1871–1874.

[7] B. Fernando et al. "Unsupervised visual domain adaptation using subspace alignment". In: *IEEE International Conference on Computer Vision (ICCV)* (2013).

[8] David J. Fleet and Yair Weiss. "Optical Flow Estimation". In: ().

[9] Y. Ganin et al. "Domain-Adversarial Training of Neural Networks". In: *Journal of Machine Learning Research* 17 (2016).

[10] Wenshuo Gao et al. "An improved Sobel edge detection". In: *Computer Science and Information Technology (ICCSIT), 2010 3rd IEEE International Conference on*. Vol. 5. IEEE. 2010, pp. 67–71.

[11] Ian Goodfellow, Yoshua Bengio, and Aaron Courville. *Deep Learning*. http://www.deeplearningbook.org. MIT Press, 2016.

[12] *Grad-CAM Torch7 Implementation*. 2016. URL: https://github.com/ramprs/grad-cam.

[13] Kaiming He et al. "Spatial Pyramid Pooling in Deep Convolutional Networks for Visual Recognition". In: *CoRR* abs/1406.4729 (2014). URL: http://arxiv.org/abs/1406.4729.

[14] P. Jackson. *Introduction to expert systems.* Addison-Wesley Pub. Co.,Reading, MA, 1986.

[15] Jing Jiang. "A Literature Survey on Domain Adaptation of Statistical Classifiers". In: (2008).

[16] Diederik P. Kingma and Jimmy Ba. "Adam: A Method for Stochastic Optimization". In: *CoRR* abs/1412.6980 (2014). URL: http://arxiv.org/abs/1412.6980.

[17] Van Der Maaten L. and Hinton GE. "Visualizing High-Dimensional Data Using t-SNE". In: *Journal of Machine Learning Research* 9 (2008). URL: http://prlab.tudelft.nl/content/visualizing-high-dimensional-data-using-t-sne.

[18] Y. LeCun et al. "Backpropagation Applied to Handwritten Zip Code Recognition". In: *Neural Computation* 1.4 (1989), pp. 541–551.

[19] Yann Lecun, Yoshua Bengio, and Geoffrey Hinton. "Deep learning". In: *Nature* 521.7553 (May 2015), pp. 436–444. ISSN: 0028-0836. DOI: 10.1038/nature14539.

[20] Jawad Nagi et al. "Max-pooling convolutional neural networks for vision-based hand gesture recognition". In: *Signal and Image Processing Applications (ICSIPA), 2011 IEEE International Conference on.* IEEE. 2011, pp. 342–347.

[21] Y. Nesterov. "A method of solving a convex programming problem with convergence rate $\mathrm{O}(1/\mathrm{k}^2)$". In: *Soviet Mathematics Doklady* 27 (1983).

[22] Eunbyung Park et al. "Combining multiple sources of knowledge in deep CNNs for action recognition". In: *2016 IEEE Winter Conference on Applications of Computer Vision, WACV 2016.* Institute of Electrical and Electronics Engineers Inc., May 2016. DOI: 10.1109/WACV.2016.7477589.

[23] David E. Rumelhart, Geoffrey E. Hinton, and Ronald J. Williams. "Learning representations by back-propagating errors". In: *Nature* 323 (1986).

[24] K. Saenko et al. "Adapting visual category models to new domains." In: *Proc. ECCV.* 2010.

[25] Dominik Scherer, Andreas Müller, and Sven Behnke. “Evaluation of pooling operations in convolutional architectures for object recognition”. In: *Artificial Neural Networks–ICANN 2010* (2010), pp. 92–101.

[26] Dominik Scherer, Andreas Müller, and Sven Behnke. “Evaluation of Pooling Operations in Convolutional Architectures for Object Recognition”. In: *Proceedings of the 20th International Conference on Artificial Neural Networks: Part III*. ICANN’10. Thessaloniki, Greece: Springer-Verlag, 2010, pp. 92–101. ISBN: 3-642-15824-2, 978-3-642-15824-7. URL: http://dl.acm.org/citation.cfm?id=1886436.1886447.

[27] Ramprasaath R. Selvaraju et al. “Grad-CAM: Why did you say that? Visual Explanations from Deep Networks via Gradient-based Localization”. In: *CoRR* abs/1610.02391 (2016). URL: http://arxiv.org/abs/1610.02391.

[28] Hidetoshi Shimodaira. “Improving predictive inference under covariate shift by weighting the log-likelihood function”. In: *Journal of Statistical Planning and Inference* 90 (2000).

[29] Karen Simonyan and Andrew Zisserman. “Very Deep Convolutional Networks for Large-Scale Image Recognition”. In: *CoRR* abs/1409.1556 (2014). URL: http://arxiv.org/abs/1409.1556.

[30] Jost Tobias Springenberg et al. “Striving for Simplicity: The All Convolutional Net”. In: *CoRR* abs/1412.6806 (2014). URL: http://arxiv.org/abs/1412.6806.

[31] Ilya Sutskever et al. “On the importance of initialization and momentum in deep learning”. In: *Proceedings of the 30th International Conference on Machine Learning*. Ed. by Sanjoy Dasgupta and David McAllester. Vol. 28. Proceedings of Machine Learning Research 3. Atlanta, Georgia, USA: PMLR, 2013, pp. 1139–1147. URL: http://proceedings.mlr.press/v28/sutskever13.html.

[32] *The iCub World Dataset*. 2013. URL: https://robotology.github.io/iCubWorld/#icubworld-transformations-modal.

[33] *The ImageNet Dataset*. 2017. URL: http://www.image-net.org/.

[34] T. Tommasi and B. Caputo. “Frustratingly Easy NBNN Domain Adaptation”. In: *IEEE International Conference on Computer Vision (ICCV)* (2013).

[35] Vladimir N. Vapnik. *Statistical Learning Theory*. Wiley-Interscience, 1998.

[36] Matthew D. Zeiler and Rob Fergus. “Visualizing and Understanding Convolutional Networks”. In: *CoRR* abs/1311.2901 (2013). URL: http://arxiv.org/abs/1311.2901.

[37] Chiyuan Zhang et al. “Understanding deep learning requires rethinking generalization”. In: *CoRR* abs/1611.03530 (2016). URL: http://arxiv.org/abs/1611.03530.